Frontiers of Information Technology & Electronic Engineering
www.jzus.zju.edu.cn; engineering.cae.cn; www.springerlink.com
ISSN 2095-9184 (print); ISSN 2095-9230 (online)
E-mail: jzus@zju.edu.cn

Synchronization of two different chaotic systems using Legendre polynomials with applications in secure communications

Saeed KHORASHADIZADEH, Mohammad-Hassan MAJIDI†‡

Faculty of Electrical and Computer Engineering, University of Birjand, Birjand 97175/376, Iran

†E-mail: m.majidi@birjand.ac.ir

Received Dec. 14, 2016; Revision accepted Mar. 7, 2017; Crosschecked Sept. 9, 2018

Abstract: In this study, a new controller for chaos synchronization is proposed. It consists of a state feedback controller and a robust control term using Legendre polynomials to compensate for uncertainties. The truncation error is also considered. Due to the orthogonal functions theorem, Legendre polynomials can approximate nonlinear functions with arbitrarily small approximation errors. As a result, they can replace fuzzy systems and neural networks to estimate and compensate for uncertainties in control systems. Legendre polynomials have fewer tuning parameters than fuzzy systems and neural networks. Thus, their tuning process is simpler. Similar to the parameters of fuzzy systems, Legendre coefficients are estimated online using the adaptation rule obtained from the stability analysis. It is assumed that the master and slave systems are the Lorenz and Chen chaotic systems, respectively. In secure communication systems, observer-based synchronization is required since only one state variable of the master system is sent through the channel. The use of observer-based synchronization to obtain other state variables is discussed. Simulation results reveal the effectiveness of the proposed approach. A comparison with a fuzzy sliding mode controller shows that the proposed controller provides a superior transient response. The problem of secure communications is explained and the controller performance in secure communications is examined.

Key words: Observer-based synchronization; Chaotic systems; Legendre polynomials; Secure communications
https://doi.org/10.1631/FITEE.1601814 **CLC number:** TN919; O415

1 Introduction

Chaos is an interesting phenomenon that has been witnessed in various fields such as fluid dynamics, mechanical systems, electrical circuits, chemical reactions, and weather forecasting. Chaos can be considered a special case of nonlinear dynamics that shows high complexity (Grzybowski et al., 2009). Due to the high sensitivity to initial conditions, predicting the behavior of a chaotic system is a challenging task. Nowadays, chaotic behavior has widespread applications in electrical and communication engineering. Chaos synchronization is important in secure communications, in which a controller is needed to reduce the synchronization error between the master and slave oscillators. Also, in the encryption process of secure communication systems, chaotic electrical circuits are used to produce random signals.

The idea of chaos synchronization using the concept of master-slave (drive-response) systems was proposed by Pecora and Carroll (1991). Based on this idea, various synchronization approaches have been proposed, such as linear and nonlinear feedback control (Yassen, 2005; Effa et al., 2009), lag synchronization (Wang and Chen, 2006), back-stepping design (Laoye et al., 2009), and sliding mode control (Li XR et al., 2005; Naseh and Haeri, 2009; Li LL et al., 2014). Several observer-based synchronization algorithms based on nonlinear observers have been presented (Grassi and Mascolo, 1997, 1998; Pogromsky

‡ Corresponding author
ORCID: Saeed KHORASHADIZADEH, http://orcid.org/0000-0003-0192-3678

and Nijmeijer, 1998; Cherrier et al., 2006; Bagheri et al., 2015; Yang et al., 2015). Various adaptive and robust control strategies have been applied to chaos synchronization (Wang and Ge, 2001; Lu et al., 2004; Shen et al., 2006; Nijsure et al., 2016; Wang et al., 2016). Dealing with channel distortion in chaos-based secure communications using particle filters has been studied (Shi et al., 2008, 2013). Also, intelligent approaches, such as fuzzy systems and neural networks, have been used in the field of chaos synchronization (Lee et al., 2008; Liu and Zhang, 2008; Chen, 2009; Hsu, 2011; Lin et al., 2015). Neuro-fuzzy systems exhibit some outstanding features, making them excellent options for uncertainty estimation and compensation. Their main characteristics are universal approximation and linear parameterization. Fuzzy systems with Gaussian membership functions (Wang, 1997) and some neural networks, such as multi-layer perceptron (MLP) and radial basis functions networks (RBFN) (Gupta et al., 2005), are universal approximators and can approximate nonlinear functions with arbitrarily small errors. The output of fuzzy systems and neural networks can be represented by the product of two vectors or matrices, one including the adjustable parameters and the other including membership functions of the fuzzy systems or activation functions of the neural network (Fateh and Khorashadizadeh, 2012a; Fateh et al., 2014a, 2014b). This form of representation considerably simplifies the stability analysis.

In addition to the aforementioned advantages, there are some disadvantages in applying neuro-fuzzy systems to controller design. Sometimes, obtaining a satisfactory fuzzy controller for a complicated system requires the knowledge of some experts specialized in that field. Without this vital information, designing a proper fuzzy controller may be a tedious task due to the time-consuming trial-and-error procedures for tuning the parameters of the fuzzy system (Khorashadizadeh and Fateh, 2015; Khorashadizadeh and Mahdian, 2016). Although all the unknown parameters of the neuro-fuzzy controller can be calculated automatically using the adaptation rules, their initial conditions and learning rates (convergence rates) are selected in advance, which considerably influences the controller performance. As a result, there are different adaptation rules for unknown parameters of a neuro-fuzzy controller. Increasing the number of adaptation rules imposes additional computational load on the controller, which is not desirable and should be avoided.

Recently, regressor-free control of nonlinear systems, such as robot manipulators using function approximation techniques, has been presented (Huang et al., 2006; Chien and Huang, 2012; Kai and Huang, 2013; Khorashadizadeh and Fateh, 2013; Fard and Khorashadizadeh, 2015; Izadbakhsh and Khorashadizadeh, 2017; Khorashadizadeh and Fateh, 2017). In this approach, uncertainties such as the inertia matrix, Jacobian matrix, or gravity vector are estimated using Legendre polynomials. According to the orthogonal functions theorem (Kreyszig, 2007), Legendre polynomials can approximate nonlinear functions with arbitrarily small approximation errors. In other words, they are universal approximators. Consequently, they may play the role of fuzzy systems and neural networks. Similarly, they are linearly parameterized and the vector of Legendre coefficients can be calculated using adaptation rules. Legendre polynomials are simpler than neural networks and fuzzy systems since they have fewer tuning parameters. The tuning parameters of Legendre polynomials are simply their coefficients, while those of fuzzy controllers include the center and width of the Gaussian membership functions, and also the weight of each rule.

In this study, we present chaos synchronization of two different chaotic systems using Legendre polynomials. It is assumed that the master system is a Lorenz system, while the slave system is the Chen system (Kuo, 2011). Our proposed controller consists of a linear state feedback, a Legendre estimator, and a robust control term for compensation for the truncation error. The Legendre estimator is responsible for compensation for the lumped uncertainty, including parametric uncertainty and external disturbances. The state feedback gain is determined based on the pole placement algorithm (Ogata, 1995), and the Legendre coefficients adaptation rule and its additional term are calculated based on stability analysis. Since in secure communication systems only one state of the master chaotic system is sent through the channel, observer-based synchronization is required. Thus, in this study, observer-based chaos synchronization using Legendre polynomials is proposed. The role of Legendre polynomials in the observer is to overcome external disturbances. In simulations, the performance of the proposed synchronization is tested first. Also, a comparison between the proposed method and a fuzzy sliding mode controller (Kuo, 2011) is performed. Then the problem of secure communications is explained and the effectiveness of the synchronization algorithm in recovering the message signal is examined.

2 System and problem description

As mentioned above, it is assumed that the master and slave systems are two different chaotic systems. A Lorenz system is defined as the master system as follows:

$$\begin{cases}\dot{x}_1 = a_1(x_2 - x_1),\\ \dot{x}_2 = b_1x_1 - x_1x_3 - x_2,\\ \dot{x}_3 = x_1x_2 - c_1x_3.\end{cases} \tag{1}$$

Suppose that the following Chen system (Effa et al., 2009) is defined as the slave system:

$$\begin{cases}\dot{y}_1 = a_2(y_2 - y_1) + d_1(t) + u_1,\\ \dot{y}_2 = (b_2 - a_2)y_1 - y_1y_3 + b_2y_2 + d_2(t) + u_2,\\ \dot{y}_3 = y_1y_2 - c_2y_3 + d_3(t) + u_3,\end{cases} \tag{2}$$

where u_1, u_2, and u_3 are the control inputs attached to the slave system and d_1, d_2, and d_3 are zero-mean Gaussian noises applied to the slave system. The parameters of the Lorenz system are set to a_1=10, b_1=28, and c_1=8/3, and the parameters of the Chen system to a_2=35, b_2=28, and c_2=3 (Kuo, 2011). Let $\boldsymbol{X}=[x_1, x_2, x_3]^{\mathrm{T}}$. Thus, Eq. (1) can be given as the following state space representation:

$$\begin{gathered}\dot{\boldsymbol{X}} = \boldsymbol{AX} + f(\boldsymbol{X}),\\ \boldsymbol{A} = \begin{bmatrix}-a_1 & a_1 & 0\\ b_1 & -1 & 0\\ 0 & 0 & -c_1\end{bmatrix}, f(\boldsymbol{X}) = \begin{bmatrix}0\\ -x_1x_3\\ x_1x_2\end{bmatrix}.\end{gathered} \tag{3}$$

Also, define $\boldsymbol{Y}=[y_1, y_2, y_3]^{\mathrm{T}}$. Eq. (2) can be given as the following state space representation:

$$\begin{gathered}\dot{\boldsymbol{Y}} = (\boldsymbol{A} + \Delta\boldsymbol{A})\boldsymbol{Y} + f(\boldsymbol{Y}) + \boldsymbol{Bu} + \boldsymbol{d},\\ \Delta\boldsymbol{A} = \begin{bmatrix}-(a_2 - a_1) & (a_2 - a_1) & 0\\ b_2 - b_1 - a_2 & b_2 + 1 & 0\\ 0 & 0 & -(c_2 - c_1)\end{bmatrix},\\ f(\boldsymbol{Y}) = \begin{bmatrix}0\\ -y_1y_3\\ y_1y_2\end{bmatrix}, \boldsymbol{B} = \boldsymbol{I}_3, \boldsymbol{u} = \begin{bmatrix}u_1\\ u_2\\ u_3\end{bmatrix}, \boldsymbol{d} = \begin{bmatrix}d_1\\ d_2\\ d_3\end{bmatrix},\end{gathered} \tag{4}$$

where $\boldsymbol{I}_3\in\mathbb{R}^{3\times3}$ is an identity matrix. Define the synchronization error as $\boldsymbol{E}=\boldsymbol{Y}-\boldsymbol{X}$. Using Eqs. (3) and (4), one can obtain

$$\dot{\boldsymbol{E}} = \boldsymbol{AE} + \Delta\boldsymbol{AY} + f(\boldsymbol{Y}) - f(\boldsymbol{X}) + \boldsymbol{Bu} + \boldsymbol{d}. \tag{5}$$

3 Legendre polynomials and function approximation

In a three-dimensional Cartesian coordinate, we can represent any arbitrary vector as a linear combination of unit vectors $\boldsymbol{i}=[1, 0, 0]^{\mathrm{T}}$, $\boldsymbol{j}=[0, 1, 0]^{\mathrm{T}}$, and $\boldsymbol{k}=[0, 0, 1]^{\mathrm{T}}$, since they are linearly independent and mutually orthogonal, due to the dot product which is generally an inner product. This idea can be simply extended to the space of nonlinear functions, which results in an interesting technique for function approximation. Consider a typical inner product as given by Khorashadizadeh and Fateh (2015):

$$\langle f, g\rangle = \int f^*(x)g(x)\mathrm{d}x, \tag{6}$$

where $f^*(x)$ is the complex conjugate of the function $f(x)$. If the inner product in Eq. (6) is zero for $f(x)\neq g(x)$, the functions $f(x)$ and $g(x)$ are called orthogonal. Suppose that V is the space of all real-valued continuous-time functions. According to Kreyszig (2007), a function $h(x)$ defined on the interval $[x_1, x_2]$ in this space can be represented as

$$h(x) = \sum_{i=1}^{m} a_i\varphi_i(x) + \varepsilon_m(x), \tag{7}$$

where the set $\{\varphi_1(x), \varphi_2(x), \ldots, \varphi_m(x)\}$ forms an orthogonal basis and $\varepsilon_m(x)$ is the approximation error. The coefficient a_i is calculated by

$$a_i = \frac{1}{A_i}\int_{x_1}^{x_2} h(x)\varphi_i(x)\mathrm{d}x,\ i = 0, 1, \cdots, m, \tag{8}$$

$$\int_{x_1}^{x_2} \varphi_i(x)\varphi_j(x)\mathrm{d}x = \begin{cases} 0,\ i \neq j, \\ A_i, i = j. \end{cases} \tag{9}$$

The approximation error $\varepsilon_m(x)$ is bounded in the sense that (Kreyszig, 2007)

$$\lim_{m\to\infty}\int_{x_1}^{x_2} \varepsilon_m^2(x)\mathrm{d}x = 0. \tag{10}$$

Considering the interval [−1, 1] and the inner product in Eq. (6), the Legendre polynomials, defined as

$$\varphi_0(x) = 1, \tag{11}$$

$$\varphi_1(x) = x, \tag{12}$$

$$(i+1)\varphi_{i+1}(x) = (2i+1)x\varphi_i(x) - i\varphi_{i-1}(x),\quad i = 1, 2, \cdots, m-1, \tag{13}$$

form an orthogonal basis (Kreyszig, 2007). Thus, a function $h(x)$ defined on the interval [−1, 1] can be approximated using Legendre polynomials (Eq. (7)) where the coefficients a_i (i=0, 1, …, m) are calculated according to Eqs. (8) and (9) and the polynomials $\varphi_i(x)$ (i=0, 1, …, m) are given by Eqs. (11)–(13). Thus,

$$h_{\mathrm{LP}}(x) = \sum_{i=1}^{m} a_i\varphi_i(x) = \boldsymbol{\alpha}^{\mathrm{T}}\boldsymbol{\varphi} \tag{14}$$

is the Legendre polynomial approximation of the function $h(x)$ where

$$\boldsymbol{\alpha} = \left[a_0, a_1, \cdots, a_m\right]^{\mathrm{T}}, \tag{15}$$

$$\boldsymbol{\varphi} = \left[\varphi_0, \varphi_1, \cdots, \varphi_m\right]^{\mathrm{T}}. \tag{16}$$

In other words, $h(x)$ can be represented as

$$h(x) = \boldsymbol{\alpha}^{\mathrm{T}}\boldsymbol{\varphi} + \varepsilon_m. \tag{17}$$

Remark 1 The most important problem in applying orthogonal functions to control systems is that the function $h(x)$ is not available. Thus, the coefficients a_i cannot be calculated according to Eqs. (8) and (9). In control systems, these coefficients are adjusted online using adaptation laws derived from stability analysis (Khorashadizadeh and Fateh, 2015). In Section 5, this issue will be explained in detail.

Remark 2 Another important issue about using orthogonal functions for function approximation in control systems is the fact that the functions $\varphi_i(x)$ are mutually orthogonal only within the interval [−1, 1]. Outside this interval, $\varphi_i(x)$ may not be mutually orthogonal. However, the uncertain functions which should be estimated in robust and adaptive control systems are generally functions of the variable time, which may increase to infinity and cannot be limited to the interval [−1, 1]. To solve this problem, we can let x=sin(ωt), in which ω is a predefined constant (Khorashadizadeh and Fateh, 2015).

4 The proposed method

In this section, two cases are discussed. First, a synchronization controller using Legendre polynomials for uncertainty estimation is presented. Note that this proposed controller cannot be applied in secure communications, since it requires all the state variables. Then to solve this problem, an observer-based approach using Legendre polynomials is presented.

4.1 Synchronization controller

The control law consists of a state feedback and an uncertainty estimator using Legendre polynomials. In other words,

$$\boldsymbol{u} = -\boldsymbol{kE} - \hat{\boldsymbol{f}} - \boldsymbol{u}_{\mathrm{r}}, \tag{18}$$

where $\boldsymbol{k}$ is the matrix of feedback gains and is designed using the pole placement algorithm such that all the eigenvalues of matrix $\boldsymbol{A}_{\mathrm{c}}$=$\boldsymbol{A}$−$\boldsymbol{Bk}$ are placed at some predefined desired points. The calculation of the controllability matrix pair ($\boldsymbol{A}$, $\boldsymbol{B}$) shows that the system is controllable and thus, we can find a gain matrix $\boldsymbol{k}$ to place the poles of the closed-loop system in desired positions. $\boldsymbol{A}$ and $\boldsymbol{B}$ are defined in Eqs. (3) and (4), respectively. The function $\hat{\boldsymbol{f}}$ is our uncertainty estimator using the first m terms of Legendre polynomials, and $\boldsymbol{u}_{\mathrm{r}}$ is considered for compensation for the truncation error. Suppose that the first five polynomials are selected. Accordingly, $\hat{\boldsymbol{f}}$ is of the form

$$\hat{\boldsymbol{f}} = \boldsymbol{\varphi}\hat{\boldsymbol{\theta}}, \tag{19}$$

where

$$\boldsymbol{\varphi} = \begin{bmatrix} \boldsymbol{\varphi}_0 & \mathbf{0} & \mathbf{0} \\ \mathbf{0} & \boldsymbol{\varphi}_0 & \mathbf{0} \\ \mathbf{0} & \mathbf{0} & \boldsymbol{\varphi}_0 \end{bmatrix},\ \boldsymbol{\varphi}_0 = [1,\ l_1,\ l_2,\ l_3,\ l_4]. \tag{20}$$

In Eq. (20), we have $l_1=x$, $l_2=(3x^2-1)/2$, $l_3=(5x^3-3x)/2$, and $l_4=(35x^4-30x^2+3)/8$. It should be emphasized that each zero in Eq. (20) is a 1×5 zero vector and $x=\sin(\omega t)$. The vector $\hat{\boldsymbol{\theta}}$ in Eq. (19) is of the form

$$\begin{aligned} &\hat{\boldsymbol{\theta}} = \left[\hat{\boldsymbol{\theta}}_1^{\mathrm{T}}, \hat{\boldsymbol{\theta}}_2^{\mathrm{T}}, \hat{\boldsymbol{\theta}}_3^{\mathrm{T}}\right]^{\mathrm{T}}, \\ &\hat{\boldsymbol{\theta}}_i = \left[a_{0i}, a_{1i}, a_{2i}, a_{3i}, a_{4i}\right]^{\mathrm{T}},\ i=1,2,3, \end{aligned} \tag{21}$$

where a_{0i}, a_{1i}, …, a_{4i} are the Legendre coefficients. The Legendre coefficients are unknown and will be estimated using the adaptation law obtained from the stability analysis in the next section. Substitution of the control law (18) into Eq. (5) results in the following closed-loop system:

$$\dot{\boldsymbol{E}} = \boldsymbol{A}\boldsymbol{E} + \boldsymbol{B}(-\boldsymbol{k}\boldsymbol{E} - \hat{\boldsymbol{f}} - \boldsymbol{u}_{\mathrm{r}}) + F(t), \tag{22}$$

where $F(t)=f(\boldsymbol{Y})-f(\boldsymbol{X})+\Delta\boldsymbol{A}\boldsymbol{Y}+\boldsymbol{d}(t)$ is the vector of lumped uncertainty and $\boldsymbol{d}(t)$ is a zero-mean Gaussian noise. Suppose that $F(t)$ can be approximated using Legendre polynomials as

$$F(t) = \boldsymbol{\varphi}\boldsymbol{\theta}^* + \boldsymbol{\varDelta}(t), \tag{23}$$

where $\boldsymbol{\theta}^*$ is the optimal bounded value of $\hat{\boldsymbol{\theta}}$ that yields the minimum approximation error (truncation error) of $\boldsymbol{\varDelta}(t)$. In fact, the control term $\boldsymbol{u}_{\mathrm{r}}$ in the control law (18) is responsible for compensation for the truncation error $\varDelta(t)$. It is assumed that $\varDelta(t)$ is bounded as $\|\boldsymbol{\varDelta}(t)\|\le\rho$ where ρ is a known constant. According to Eqs. (19) and (23), and using the definition $\boldsymbol{A}_{\mathrm{c}}=\boldsymbol{A}-\boldsymbol{B}\boldsymbol{k}$, we can rewrite Eq. (22) as

$$\dot{\boldsymbol{E}} = \boldsymbol{A}_{\mathrm{c}}\boldsymbol{E} + \boldsymbol{B}(\boldsymbol{\varphi}\tilde{\boldsymbol{\theta}} - \boldsymbol{u}_{\mathrm{r}} + \boldsymbol{\varDelta}(t)), \tag{24}$$

where $\tilde{\boldsymbol{\theta}} = \boldsymbol{\theta}^* - \hat{\boldsymbol{\theta}}$.

4.2 Observer-based secure communication

In observer-based secure communication systems, only one state variable is sent through the communication channel, and instead of a slave chaotic system on the receiver side, an observer is used to estimate the required signals to perform the decryption process. Consider the following master system (Liao and Tsai, 2000):

$$\dot{\boldsymbol{X}} = \boldsymbol{A}\boldsymbol{X} + f(\boldsymbol{y}) + \boldsymbol{B}\boldsymbol{d}(t), \tag{25}$$

where $\boldsymbol{y}=[1,\ 0,\ 0]\boldsymbol{X}=\boldsymbol{C}\boldsymbol{X}$ is the master output that is sent to the channel, $f(\boldsymbol{y})$ is a real analytic vector, and $\boldsymbol{d}(t)$ is the bounded external disturbance. According to Eq. (23), it is assumed that $\boldsymbol{d}(t)=\boldsymbol{\varphi}\boldsymbol{\theta}^*+\boldsymbol{\varDelta}(t)$. Now, consider the following observer:

$$\dot{\hat{\boldsymbol{X}}} = \boldsymbol{A}\hat{\boldsymbol{X}} + \boldsymbol{L}(\boldsymbol{y}-\hat{\boldsymbol{y}}) + f(\boldsymbol{y}) + \boldsymbol{B}(\boldsymbol{\varphi}\hat{\boldsymbol{\theta}} + \boldsymbol{u}_{\mathrm{r}}), \tag{26}$$

where $\hat{\boldsymbol{X}}$ is the observer state vector, $\boldsymbol{L}$ is a gain matrix obtained by the pole placement approach to set the observer poles at desired values, $\boldsymbol{\varphi}\hat{\boldsymbol{\theta}}$ is the uncertainty estimator using Legendre polynomials (Eqs. (19)–(21)) to compensate for the external disturbance $\boldsymbol{d}$, and $\boldsymbol{u}_{\mathrm{r}}$ is designed to compensate for the truncation error of the Legendre polynomials. Using Eqs. (25), (26), and Eqs. (19)–(23), the observer error dynamics is given by

$$\dot{\hat{\boldsymbol{E}}} = \boldsymbol{A}_{\mathrm{o}}\hat{\boldsymbol{E}} + \boldsymbol{B}(\boldsymbol{\varphi}\tilde{\boldsymbol{\theta}} - \boldsymbol{u}_{\mathrm{r}} + \boldsymbol{\varDelta}(t)), \tag{27}$$

where $\boldsymbol{A}_{\mathrm{o}}=\boldsymbol{A}-\boldsymbol{L}\boldsymbol{C}$ and $\hat{\boldsymbol{E}} = \boldsymbol{X} - \hat{\boldsymbol{X}}$ is the observer error vector.

5 Stability analysis

In this section, a Lyapunov-based proof for asymptotic convergence of the synchronization error to zero is presented. The same proof can be followed for observer-based secure communications.

To prove chaos synchronization using the proposed controller, consider the following Lyapunov function candidate:

$$V=\frac{1}{2}\boldsymbol{E}^{\mathrm{T}}\boldsymbol{P}\boldsymbol{E}+\frac{1}{2\gamma}\tilde{\boldsymbol{\theta}}^{\mathrm{T}}\tilde{\boldsymbol{\theta}}, \tag{28}$$

where $\boldsymbol{P}$ is a symmetric positive definite matrix satisfying the Lyapunov equation (Slotine and Li, 1991):

$$\boldsymbol{A}_{\mathrm{c}}^{\mathrm{T}}\boldsymbol{P}+\boldsymbol{P}\boldsymbol{A}_{\mathrm{c}}=-\boldsymbol{Q}, \tag{29}$$

where $\boldsymbol{Q}$ is a positive definite matrix selected by the designer, and γ is a positive constant. The time derivative of V is given by

$$\dot{V}=\frac{1}{2}(\dot{\boldsymbol{E}}^{\mathrm{T}}\boldsymbol{P}\boldsymbol{E}+\boldsymbol{E}^{\mathrm{T}}\boldsymbol{P}\dot{\boldsymbol{E}})-\frac{1}{\gamma}\tilde{\boldsymbol{\theta}}^{\mathrm{T}}\dot{\hat{\boldsymbol{\theta}}}. \tag{30}$$

Substituting $\dot{\boldsymbol{E}}$ from Eq. (24) into Eq. (30) with some simple manipulations results in

$$\begin{aligned}\dot{V}=&-\frac{1}{2}\boldsymbol{E}^{\mathrm{T}}\boldsymbol{Q}\boldsymbol{E}+\tilde{\boldsymbol{\theta}}^{\mathrm{T}}\boldsymbol{\varphi}^{\mathrm{T}}\boldsymbol{B}^{\mathrm{T}}\boldsymbol{P}\boldsymbol{E}\\&+\boldsymbol{E}^{\mathrm{T}}\boldsymbol{P}\boldsymbol{B}(\boldsymbol{\varDelta}-\boldsymbol{u}_{\mathrm{r}})-\frac{1}{\gamma}\tilde{\boldsymbol{\theta}}^{\mathrm{T}}\dot{\hat{\boldsymbol{\theta}}}.\end{aligned} \tag{31}$$

Assume that

$$\dot{\hat{\boldsymbol{\theta}}}=\gamma\boldsymbol{\varphi}^{\mathrm{T}}\boldsymbol{B}^{\mathrm{T}}\boldsymbol{P}\boldsymbol{E}. \tag{32}$$

Then Eq. (31) can be rewritten as

$$\dot{V}=-\frac{1}{2}\boldsymbol{E}^{\mathrm{T}}\boldsymbol{Q}\boldsymbol{E}+\boldsymbol{E}^{\mathrm{T}}\boldsymbol{P}\boldsymbol{B}(\boldsymbol{\varDelta}(t)-\boldsymbol{u}_{\mathrm{r}}). \tag{33}$$

If we propose $\boldsymbol{u}_{\mathrm{r}}$ such that

$$\boldsymbol{E}^{\mathrm{T}}\boldsymbol{P}\boldsymbol{B}(\boldsymbol{\varDelta}(t)-\boldsymbol{u}_{\mathrm{r}})\le 0, \tag{34}$$

then $\dot{V}\le 0$ is satisfied. To this end, suppose that $\boldsymbol{u}_{\mathrm{r}}$ is of the form

$$\boldsymbol{u}_{\mathrm{r}}=\rho\,\mathrm{sign}(\boldsymbol{E}^{\mathrm{T}}\boldsymbol{P}\boldsymbol{B}). \tag{35}$$

Now, it shows that this $\boldsymbol{u}_{\mathrm{r}}$ can satisfy inequality (34). Substituting Eq. (35) into inequality (34) yields

$$\boldsymbol{E}^{\mathrm{T}}\boldsymbol{P}\boldsymbol{\varDelta}(t)-\boldsymbol{E}^{\mathrm{T}}\boldsymbol{P}\rho\,\mathrm{sign}(\boldsymbol{E}^{\mathrm{T}}\boldsymbol{P})\le 0. \tag{36}$$

To ensure that inequality (36) is satisfied, we guarantee that

$$\|\boldsymbol{E}^{\mathrm{T}}\boldsymbol{P}\boldsymbol{B}\|\|\boldsymbol{\varDelta}(t)\|-\rho\|\boldsymbol{E}^{\mathrm{T}}\boldsymbol{P}\boldsymbol{B}\|\le 0. \tag{37}$$

In other words,

$$\|\boldsymbol{E}^{\mathrm{T}}\boldsymbol{P}\boldsymbol{B}\|(\|\boldsymbol{\varDelta}(t)\|-\rho)\le 0. \tag{38}$$

Since we have assumed that $\|\boldsymbol{\varDelta}(t)\|\le\rho$, inequality (38) is always true and $\dot{V}\le 0$ is satisfied. Consequently, $\boldsymbol{E}$ and $\tilde{\boldsymbol{\theta}}$ are bounded (Slotine and Li, 1991), and we have

$$V(\tilde{\boldsymbol{\theta}}(t),\boldsymbol{E}(t))\le V(\tilde{\boldsymbol{\theta}}(0),\boldsymbol{E}(0)). \tag{39}$$

As a result, $\hat{\boldsymbol{\theta}}$ is also bounded. Therefore, the control signal in Eq. (18) and $\dot{\boldsymbol{E}}$ in Eq. (24) are bounded. Define $\varOmega(t)=0.5\boldsymbol{E}^{\mathrm{T}}\boldsymbol{Q}\boldsymbol{E}$. It is obvious that $\varOmega(t)\le-\dot{V}$. Integrating it with respect to time yields

$$\int_0^t\varOmega(\tau)\mathrm{d}\tau\le V(\tilde{\boldsymbol{\theta}}(0),\boldsymbol{E}(0))-V(\tilde{\boldsymbol{\theta}}(t),\boldsymbol{E}(t)). \tag{40}$$

Because $V(\tilde{\boldsymbol{\theta}}(0),\boldsymbol{E}(0))$ is bounded and $V(\tilde{\boldsymbol{\theta}}(t),\boldsymbol{E}(t))$ is non-increasing and bounded, the following result is obtained (Khorashadizadeh and Fateh, 2013):

$$\lim_{t\to\infty}\int_0^t\varOmega(\tau)\mathrm{d}\tau\le\infty. \tag{41}$$

As mentioned above, $\dot{\boldsymbol{E}}$ is bounded. Thus, $\dot{\varOmega}(t)=\dot{\boldsymbol{E}}^{\mathrm{T}}\boldsymbol{Q}\boldsymbol{E}$ is also bounded. Now, Barbalat's lemma (Slotine and Li, 1991) can be applied to prove that the synchronization error $\boldsymbol{E}$ asymptotically converges to zero.

Lemma 1 (Barbalat's lemma) If $f(t)$ has a finite time limit as $t\to\infty$ and $\dot{f}(t)$ is uniformly continuous (in other words, $\ddot{f}(t)$ is bounded), then $\dot{f}(t)\to 0$ as $t\to\infty$.

Suppose that $f(t)$ in Barbalat's lemma is given by

$$f(t)=\int_0^t\varOmega(\tau)\mathrm{d}\tau. \tag{42}$$

According to inequality (41), $f(t)$ has a finite time limit as $t\to\infty$. It is obvious that

$$\ddot{f}(t)=\dot{\Omega}(t)=\dot{\boldsymbol{E}}^{\mathrm{T}}\boldsymbol{QE}. \tag{43}$$

As mentioned above, $\dot{\Omega}(t)$ is bounded, which results in the boundedness of $\ddot{f}(t)$. Therefore, it follows Barbalat's lemma that $\dot{f}(t)=\Omega(t)\to 0$ as $t\to\infty$. Therefore, the asymptotic convergence of the synchronization error is proven.

Remark 3 The observer-based synchronization can be followed similarly to prove that the observer error asymptotically converges to zero. The vector $\boldsymbol{E}$ in Eq. (28) should be changed to $\hat{\boldsymbol{E}}$, and that in Eq. (30) should be substituted by $\dot{\hat{\boldsymbol{E}}}$ from Eq. (27). Also, $\boldsymbol{A}_{\mathrm{o}}$, instead of $\boldsymbol{A}_{\mathrm{c}}$, should be used in Eq. (29).

6 Simulation results

In this section, the influence of the proposed controller using Legendre polynomials on the synchronization error is studied. Also, the estimation performance of the Legendre polynomials is investigated. Then the results of the proposed controller are compared with those of a fuzzy sliding mode synchronization controller (Kuo, 2011). Finally, the satisfactory performance of the proposed controller in a secure communication problem is verified.

6.1 Performance of the proposed controller

Consider the master and slave oscillators described in Eqs. (1) and (2) with the initial conditions of $\boldsymbol{X}(0)=[10, 10, 10]^{\mathrm{T}}$ and $\boldsymbol{Y}(0)=[2, 2, 2]^{\mathrm{T}}$. To achieve satisfactory synchronization, the feedback gain $\boldsymbol{k}$ is selected such that the eigenvalues of the matrix $\boldsymbol{A}_{\mathrm{c}}=\boldsymbol{A}-\boldsymbol{Bk}$ are placed at −64, −62, and −40. To find the desired $\boldsymbol{k}$, we can run the MATLAB command

$$\boldsymbol{k}=\mathrm{place}(\boldsymbol{A},\boldsymbol{B},[-64,-62,-40]), \tag{44}$$

resulting in

$$\boldsymbol{k}=\begin{bmatrix}54 & 10 & 0\\ 28 & 61 & 0\\ 0 & 0 & 37.33\end{bmatrix}. \tag{45}$$

If the poles are closer to the origin, the elements of the matrix $\boldsymbol{k}$ will be smaller, which results in an undesirable synchronization error. On the other hand, increasing the elements of the matrix $\boldsymbol{k}$ by using poles farther apart results in a large control input at initial times, or may lead to the chattering phenomenon. Thus, there should be a trade-off between the accuracy and the amplitude of the control signal. Suppose that the positive definite matrix $\boldsymbol{Q}$ is chosen as $\boldsymbol{Q}=400\boldsymbol{I}_3$. The reason for this large $\boldsymbol{Q}$ can be explained by Eq. (30), which shows that increasing the eigenvalues of $\boldsymbol{Q}$ results in a more negative $\dot{V}$. Consequently, the synchronization error reduces faster. To calculate the matrix $\boldsymbol{P}$ in Eq. (29), run the MATLAB command $\boldsymbol{P}$=lyap($\boldsymbol{A}_{\mathrm{c}}^{\mathrm{T}}$, $\boldsymbol{Q}$). Then we have

$$\boldsymbol{P}=\begin{bmatrix}3.125 & 0 & 0\\ 0 & 3.2258 & 0\\ 0 & 0 & 5\end{bmatrix}. \tag{46}$$

The initial values of all Legendre coefficients $\hat{\boldsymbol{\theta}}(0)$ have been set to zero. It has been assumed that the upper bound of the truncation is $\rho=0.1$. The synchronization performances for all the states are illustrated in Fig. 1. In spite of different initial conditions and different models of master and slave systems, they are synchronized rapidly when the controller is applied at t=3 s. The control signal $\boldsymbol{u}$ is given in Fig. 2. According to this figure, the control efforts are bounded without any chattering.

As mentioned above, the Legendre polynomials are responsible for estimation of the lumped uncertainty $F(t)=f(\boldsymbol{Y})-f(\boldsymbol{X})+\Delta\boldsymbol{AY}=[F_1, F_2, F_3]^{\mathrm{T}}$. The estimation performance of Legendre polynomials is shown in Fig. 3. By applying the controller, Legendre polynomials can estimate the lumped uncertainty very well. To investigate the influence of uncertainty estimation using Legendre polynomials, consider the mean squared error (MSE) criterion defined by

$$\mathrm{MSE}=\frac{1}{7}\int_3^{10}\boldsymbol{E}^{\mathrm{T}}(t)\boldsymbol{E}(t)\mathrm{d}t. \tag{47}$$

In the case of including Legendre polynomials in the control law, we have MSE=0.1667. If Legendre polynomials are omitted in the control law, we obtain MSE=2.877. Thus, uncertainty estimation using

Legendre polynomials considerably reduces the synchronization error. Optimization algorithms can be used to find the optimal values of controller parameters (Fateh and Khorashadizadeh, 2012b; Zadeh et al., 2016).

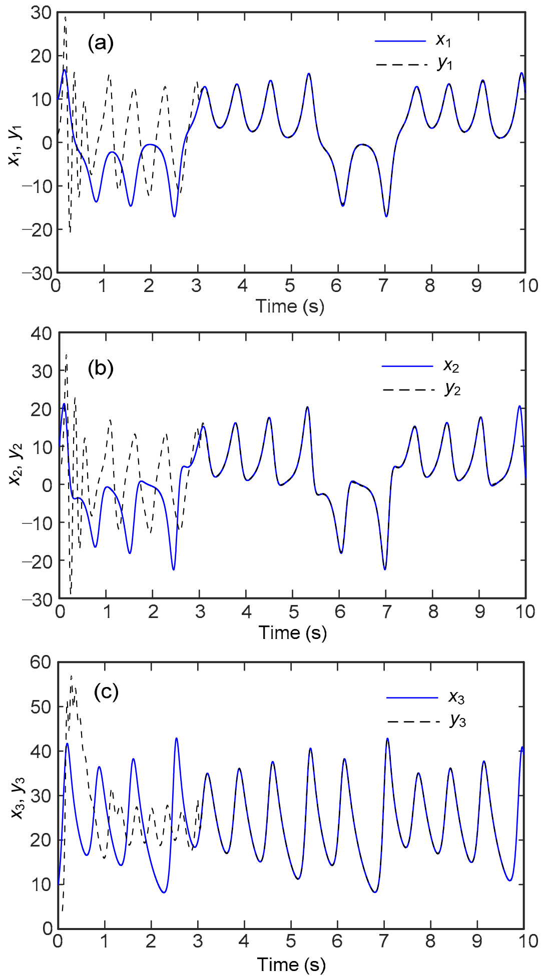

Fig. 1 Time responses of x_1 and y_1 (a), x_2 and y_2 (b), and x_3 and y_3 (c) before and after the controller is applied

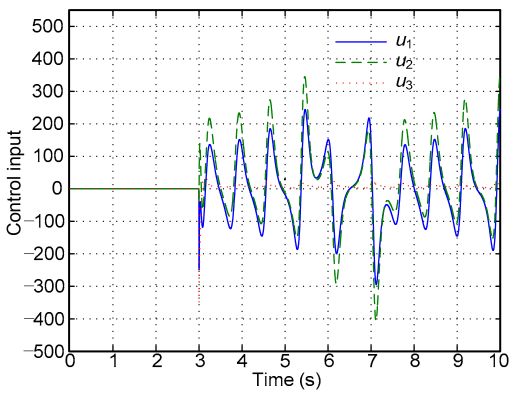

Fig. 2 Control inputs

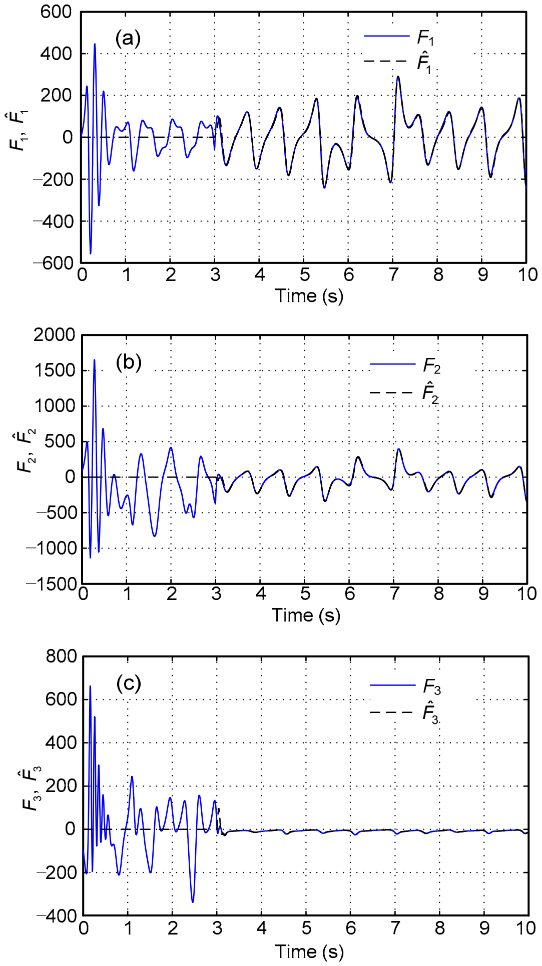

Fig. 3 Performance of Legendre polynomials in estimating F_1 (a), F_2 (b), and F_3 (c)

6.2 Comparison with a fuzzy sliding mode synchronization controller

Consider the fuzzy sliding mode synchronization controller presented by Kuo (2011). The master and slave models used in this study and their initial conditions are the same as those given by Kuo (2011). The synchronization error of the proposed controller is presented in Fig. 4. In comparison with Fig. 3c of Kuo (2011), it is obvious that our proposed controller is faster in reducing synchronization errors. After applying the controller at t=3 s, it takes about 3 s for the fuzzy sliding mode controller to reduce the synchronization error to zero, while the proposed controller is much faster. Moreover, it is clear that the design procedure of our proposed controller is simpler since it is not engaged in the determination of the parameters used in membership functions.

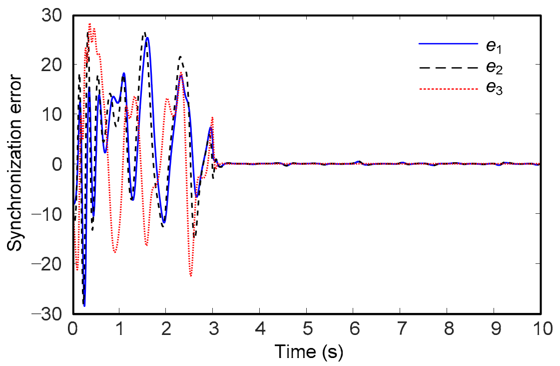

Fig. 4 Synchronization error of the proposed method

6.3 Application to secure communications (observer-based synchronization)

The procedure of secure communications is illustrated in Fig. 5. The message $m(t)$ is added to the output of the master chaotic system. We have assumed that x_1 is the master output. As a result, a new signal $\boldsymbol{y}'$ is generated in which the message is hidden. This signal is transmitted to the slave chaotic system and injected into the transmitter chaotic system. According to Liao and Tsai (2000), the transmitter (Eq. (25)) is modified as

$$\dot{\boldsymbol{X}} = \boldsymbol{AX} + f(\boldsymbol{y}') + \boldsymbol{Bd} + \boldsymbol{L}m(t),\ \ \boldsymbol{y}' = \boldsymbol{CX} + m(t). \quad (48)$$

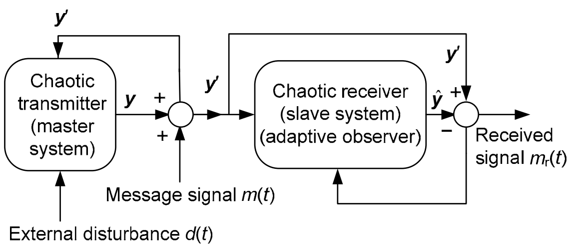

Fig. 5 Block diagram of secure communications using chaotic systems (adapted from Liao and Tsai (2000))

As a result, the observer is proposed as

$$\dot{\hat{\boldsymbol{X}}} = \boldsymbol{A}\hat{\boldsymbol{X}} + f(\boldsymbol{y}') + \boldsymbol{B}(\boldsymbol{\varphi}\hat{\boldsymbol{\theta}} + \boldsymbol{u}_{\mathrm{r}}) + \boldsymbol{L}(\boldsymbol{y}' - \hat{\boldsymbol{y}}). \quad (49)$$

As guaranteed by the stability analysis given in Section 5 and Remark 3, the observer error will converge to zero as $t\to\infty$. Then we can write

$$\begin{aligned} \lim_{t\to\infty} m_{\mathrm{r}}(t) &= \lim_{t\to\infty}(\boldsymbol{y}' - \hat{\boldsymbol{y}}) = \lim_{t\to\infty}(\boldsymbol{y} - \hat{\boldsymbol{y}} + m(t)) \\ &= \lim_{t\to\infty} m(t), \end{aligned} \quad (50)$$

which implies that the message signal will be asymptotically recovered at the receiver end. Suppose that the master system is a Chua's circuit as described by Liao and Tsai (2000):

$$\begin{cases} \dot{x}_1 = 10(x_2 - x_1 - f(x_1)) + d(t), \\ \dot{x}_2 = x_1 - x_2 + x_3, \\ \dot{x}_3 = -15x_2 - 0.385x_3, \\ y = \boldsymbol{CX} = [1,0,0]\boldsymbol{X} = x_1, \\ f(x_1) = bx_1 + 0.5(a-b)(|x_1+1| - |x_1-1|), \\ d(t) = \cos(2t). \end{cases} \quad (51)$$

Now, assume that the original message

$$m(t) = 0.1\sin(20t) \quad (52)$$

is going to be recovered using this communication system (Liao and Tsai, 2000). The desired poles for the observer (eigenvalues of $\boldsymbol{A}_{\mathrm{o}}=\boldsymbol{A}-\boldsymbol{LC}$) have been set to $\boldsymbol{p}_{\mathrm{o}}=[-50, -60, -70]$. We can run the MATLAB command place($\boldsymbol{A}^{\mathrm{T}}$, $\boldsymbol{C}^{\mathrm{T}}$, $\boldsymbol{p}_{\mathrm{o}}$) to calculate the vector $\boldsymbol{L}$. The performance of the proposed observer in recovering the message signal is shown in Fig. 6. After a transient state, the original and recovered messages are nearly the same. As shown in the magnified picture, the recovered message and the original message converge to each other within 0.1 s.

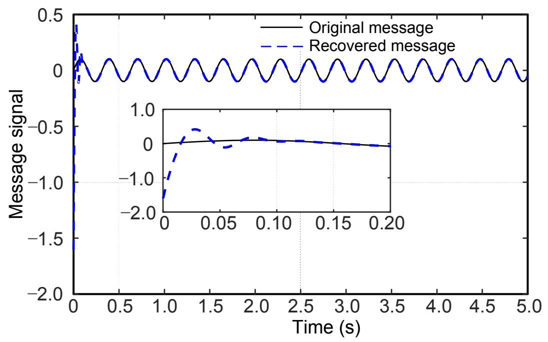

Fig. 6 Original and recovered message signals (the transient state is magnified)

7 Conclusions

A new algorithm for chaos synchronization has been proposed based on the universal approximation property of Legendre polynomials. Due to the orthogonal functions theorem, Legendre polynomials can approximate nonlinear functions with arbitrarily small approximation errors. From this point of view, Legendre polynomials are similar to neural networks and fuzzy systems. Also, observer-based chaos synchronization using Legendre polynomials has been presented and applied to secure communications. A comparison between Legendre polynomials and a fuzzy sliding mode controller showed that the proposed algorithm can reduce the synchronization error faster. Moreover, the structure of Legendre polynomials is simpler since there are fewer tuning parameters.

References

Bagheri P, Shahrokhi M, Salarieh H, 2015. Adaptive observer-based synchronization of two non-identical chaotic systems with unknown parameters. *J Vibr Contr*, 23(3): 389-399. https://doi.org/10.1177/1077546315580052

Chen CS, 2009. Quadratic optimal neural fuzzy control for synchronization of uncertain chaotic systems. *Exp Syst Appl*, 36(9):11827-11835. https://doi.org/10.1016/j.eswa.2009.04.007

Cherrier E, Boutayeb M, Ragot J, 2006. Observers-based synchronization and input recovery for a class of nonlinear chaotic models. *IEEE Trans Circ Syst I*, 53(9): 1977-1988. https://doi.org/10.1109/TCSI.2006.882817

Chien MC, Huang AC, 2012. Adaptive impedance controller design for flexible-joint electrically-driven robots without computation of the regressor matrix. *Robotica*, 30(1): 133-144. https://doi.org/10.1017/S0263574711000403

Effa JY, Essimbi BZ, Ngundam JM, 2009. Synchronization of improved chaotic Colpitts oscillators using nonlinear feedback control. *Nonl Dynam*, 58(1-2):39-48. https://doi.org/10.1007/s11071-008-9459-7

Fard MB, Khorashadizadeh S, 2015. Model free robust impedance control of robot manipulators using Fourier series expansion. AI & Robotics, p.1-7. https://doi.org/10.1109/RIOS.2015.7270740

Fateh MM, Khorashadizadeh S, 2012a. Robust control of electrically driven robots by adaptive fuzzy estimation of uncertainty. *Nonl Dynam*, 69(3):1465-1477. https://doi.org/10.1007/s11071-012-0362-x

Fateh MM, Khorashadizadeh S, 2012b. Optimal robust voltage control of electrically driven robot manipulators. *Nonl Dynam*, 70(2):1445-1458. https://doi.org/10.1007/s11071-012-0546-4

Fateh MM, Ahmadi SM, Khorashadizadeh S, 2014a. Adaptive RBF network control for robot manipulators. *J AI Data Min*, 2(2):159-166. https://doi.org/10.22044/jadm.2014.246

Fateh MM, Azargoshasb S, Khorashadizadeh S, 2014b. Model-free discrete control for robot manipulators using a fuzzy estimator. *Int J Comput Math Electr Electron Eng*, 33(3): 1051-1067. https://doi.org/10.1108/COMPEL-05-2013-0185

Grassi G, Mascolo S, 1997. Nonlinear observer design to synchronize hyperchaotic systems via a scalar signal. *IEEE Trans Circ Syst I*, 44(10):1011-1014. https://doi.org/10.1109/81.633891

Grassi G, Mascolo S, 1998. Design of nonlinear observers for hyperchaos synchronization using a scalar signal. IEEE Int Symp on Circuits and Systems, p.283-286. https://doi.org/10.1109/ISCAS.1998.704006

Grzybowski JMV, Rafikov M, Balthazar JM, 2009. Synchronization of the unified chaotic system and application in secure communication. *Commun Nonl Sci Numer Simul*, 14(6):2793-2806. https://doi.org/10.1016/j.cnsns.2008.09.028

Gupta MM, Jin L, Homma N, 2005. Static and Dynamic Neural Networks: from Fundamentals to Advanced Theory. Wiley-IEEE Press, New York, USA. https://doi.org/10.1002/0471427950

Hsu CF, 2011. Adaptive fuzzy wavelet neural controller design for chaos synchronization. *Expert Syst Appl*, 38(8): 10475-10483. https://doi.org/10.1016/j.eswa.2011.02.092

Huang AC, Wu SC, Ting WF, 2006. A FAT-based adaptive controller for robot manipulators without regressor matrix: theory and experiments. *Robotica*, 24(2):205-210. https://doi.org/10.1017/S0263574705002031

Izadbakhsh A, Khorashadizadeh S, 2017. Robust task-space control of robot manipulators using differential equations for uncertainty estimation. *Robotica*, 35(9):1923-1938. https://doi.org/10.1017/S0263574716000588

Kai CY, Huang AC, 2013. A regressor-free adaptive controller for robot manipulators without Slotine and Li's modification. *Robotica*, 31(7):105058. https://doi.org/10.1017/S0263574713000301

Khorashadizadeh S, Fateh MM, 2013. Adaptive Fourier series-based control of electrically driven robot manipulators. 3rd Int Conf on Control, Instrumentation, and Automation, p.213-218. https://doi.org/10.1109/ICCIAutom.2013.6912837

Khorashadizadeh S, Fateh MM, 2015. Robust task-space control of robot manipulators using Legendre polynomials for uncertainty estimation. *Nonl Dynam*, 79(2):1151-1161. https://doi.org/10.1007/s11071-014-1730-5

Khorashadizadeh S, Fateh MM, 2017. Uncertainty estimation in robust tracking control of robot manipulators using the Fourier series expansion. *Robotica*, 35(2):310-336. https://doi.org/10.1017/S026357471500051X

Khorashadizadeh S, Mahdian M, 2016. Voltage tracking control of DC-DC boost converter using brain emotional learning. 4th Int Conf on Control, Instrumentation, and Automation, p.268-272. https://doi.org/10.1109/ICCIAutom.2016.7483172

Kreyszig E, 2007. Advanced Engineering Mathematics. John Wiley & Sons, Hoboken, USA.

Kuo CL, 2011. Design of a fuzzy sliding-mode synchronization controller for two different chaos systems. *Comput*

Math Appl, 61(8):2090-2095.
https://doi.org/10.1016/j.camwa.2010.08.080

Laoye JA, Vincent UE, Kareem SO, 2009. Chaos control of 4D chaotic systems using recursive backstepping nonlinear controller. *Chaos Sol Fract*, 39(1):356-362.
https://doi.org/10.1016/j.chaos.2007.04.020

Lee SM, Ji DH, Park JH, et al., 2008. $\mathscr{H}_\infty$ synchronization of chaotic systems via dynamic feedback approach. *Phys Lett A*, 372(29):4905-4912.
https://doi.org/10.1016/j.physleta.2008.05.047

Li LL, Liu Y, Yao QG, 2014. Robust synchronization of chaotic systems using slidingmode and feedback control. *J Zhejiang Univ-Sci C (Comput & Electron)*, 15(3):211-222.
https://doi.org/10.1631/jzus.C1300266

Li XR, Zhao LY, Zhao GZ, 2005. Sliding mode control for synchronization of chaotic systems with structure or parameters mismatching. *J Zhejiang Univ-Sci*, 6A(6):571-576. https://doi.org/10.1631/jzus.2005.A0571

Liao TL, Tsai SH, 2000. Adaptive synchronization of chaotic systems and its application to secure communications. *Chaos Sol Fract*, 11(9):1387-1396.
https://doi.org/10.1016/S0960-0779(99)00051-X

Lin TC, Huang FY, Du ZB, et al., 2015. Synchronization of fuzzy modeling chaotic time delay memristor-based Chua's circuits with application to secure communication. *Int J Fuzzy Syst*, 17(2):206-214.
https://doi.org/10.1007/s40815-015-0024-5

Liu MQ, Zhang JH, 2008. Exponential synchronization of general chaotic delayed neural networks via hybrid feedback. *J Zhejiang Univ-Sci A*, 9(2):262-270.
https://doi.org/10.1631/jzus.A071336

Lu JA, Wu XQ, Han XP, et al., 2004. Adaptive feedback synchronization of a unified chaotic system. *Phys Lett A*, 329(4-5):327-333.
https://doi.org/10.1016/j.physleta.2004.07.024

Naseh MR, Haeri M, 2009. Robustness and robust stability of the active sliding mode synchronization. *Chaos Sol Fract*, 39(1):196-203.
https://doi.org/10.1016/j.chaos.2007.01.123

Nijsure YA, Kaddoum G, Gagnon G, et al., 2016. Adaptive air-to-ground secure communication system based on ADS-B and wide-area multilateration. *IEEE Trans Veh Technol*, 65(5):3150-3165.
https://doi.org/10.1109/TVT.2015.2438171

Ogata K, 1995. Discrete-Time Control Systems (2nd Ed.). Prentice Hall, Englewood Cliffs, USA.

Pecora LM, Carroll TL, 1991. Driving systems with chaotic signals. *Phys Rev A*, 44(4):2374-2383.
https://doi.org/10.1103/PhysRevA.44.2374

Pogromsky A, Nijmeijer H, 1998. Observer-based robust synchronization of dynamical systems. *Int J Bifurc Chaos*, 8(11):2243-2254.

Shen C, Shi ZG, Ran LX, 2006. Adaptive synchronization of chaotic Colpitts circuits against parameter mismatches and channel distortions. *J Zhejiang Univ-Sci A*, 7(S2): 228-236. https://doi.org/10.1631/jzus.2006.AS0228

Shi ZG, Hong SH, Chen JM, et al., 2008. Particle filter-based synchronization of chaotic Colpitts circuits combating AWGN channel distortion. *Circ Syst Signal Process*, 27(6):833-845.
https://doi.org/10.1007/s00034-008-9062-7

Shi ZG, Bi SJ, Zhang HT, et al., 2013. Improved auxiliary particle filter-based synchronization of chaotic Colpitts circuit and its application to secure communication. *Wirel Commun Mob Comput*, 15(10):1456-1470.
https://doi.org/10.1002/wcm.2446

Slotine JJE, Li WP, 1991. Applied Nonlinear Control. Prentice-Hall, Englewood Cliffs, USA.

Wang C, Ge SS, 2001. Adaptive backstepping control of uncertain Lorenz system. *Int J Bifurc Chaos*, 11(4):1115-1119. https://doi.org/10.1142/S0218127401002560

Wang H, Ye JM, Miao ZH, et al., 2016. Robust finite-time chaos synchronization of time-delay chaotic systems and its application in secure communication. *Trans Inst Meas Contr*, 40(4):1177-1187.
https://doi.org/10.1177/0142331216678311

Wang LX, 1997. A Course in Fuzzy Systems and Control. Prentice-Hall, New York, USA.

Wang Q, Chen Y, 2006. Generalized *Q-S* (lag, anticipated and complete) synchronization in modified Chua's circuit and Hindmarsh-Rose systems. *Appl Math Comput*, 181(1):48-56. https://doi.org/10.1016/j.amc.2006.01.017

Yang JQ, Chen YT, Zhu FL, 2015. Associated observer-based synchronization for uncertain chaotic systems subject to channel noise and chaos-based secure communication. *Neurocomputing*, 167:587-595.
https://doi.org/10.1016/j.neucom.2015.04.030

Yassen MT, 2005. Controlling chaos and synchronization for new chaotic system using linear feedback control. *Chaos Sol Fract*, 26(3):913-920.
https://doi.org/10.1016/j.chaos.2005.01.047

Zadeh SMH, Khorashadizadeh S, Fateh MM, et al., 2016. Optimal sliding mode control of a robot manipulator under uncertainty using PSO. *Nonl Dynam*, 84(4):2227-2239. https://doi.org/10.1007/s11071-016-2641-4